Pinczewski, W. V., Ph.D. thesis, Univ. of New South Wales, Australia (1973).
———, and C. J. D. Fell, "The Transition from Froth-to-Spray Regime on Commercially Loaded Sieve Trays," *Trans. Inst. Chem. Engrs.*, **50**, 102 (1972).
———, "Nature of the Two-Phase Dispersion on Sieve Plates Operating in the Spray Regime," *ibid.*, **52**, 294 (1974).
Porter, K. E., and M. J. Lockett, "Prediction of Plate Efficiency in Columns of Large Diameter," Paper presented at AIChE National Meeting, Houston, Tex. (1975).
Porter, K. E., and P. F. Y. Wong, "Transition from Spray to Bubbling on Sieve Trays," *Distillation, 1969* (London: Inst. Chem. Engrs.), **2**, 22 (1969).

Manuscript received July 7, 1975; revision received September 16 and accepted September 18, 1975.

Some Liquid Holdup Experimental Data in Trickle-Bed Reactors for Foaming and Nonfoaming Hydrocarbons

JEAN-CLAUDE CHARPENTIER and MICHEL FAVIER

Laboratoire des Sciences du Génie Chimique, CNRS
Ecole Nationale Superieure des Industries Chimiques—54042 NANCY CEDEX (France)

TABLE 1. PACKING PROPERTIES

Type	Glass spheres	Spherical catalyst	Cylindrical catalyst 1	Cylindrical catalyst 2
d, mm	3	3	1.8 × 6	1.4 × 5
ϵ, external void	0.38	0.39	0.39	0.37
a_g, m^{-1}	2,000	2,000	2,555	3,257
β_c	0.10	0.077-0.11	0.08	0.06-0.08
D, m	0.10	0.05	0.05	0.05
h_k	12.5	5.75-5.66	4	3.5
h_B	0.274	0.303-0.40	0.515	0.28

From the recent and excellent review paper written by Satterfield (1975), it appears that authors disagree on the use of predicting correlations for liquid holdup in trickle-bed reactors (Satterfield and Way, 1972; Henry and Gilbert, 1973; Mears, 1974; Wijffels et al., 1974). For this fundamental parameter for the design of such reactors, we would like to present experimental data concerning twenty gas-hydrocarbons systems with three types of cobalt/molybdenum/aluminum oxide catalyst and with glass spheres. Our aim is also to compare the fit of the different correlations to the present data and to show that predicting correlations relative to water as liquid phase may be somewhat questionable when applied to hydrocarbons.

Experiments were carried out in a 5 cm I.D. column packed to a maximum length of 1.20 m. Properties of the spherical and cylindrical catalyst packings are given in Table 1. This reactor was operated at atmospheric pressure over the range 20° to 30°C. Some results are also taken in a 10 cm I.D. column. Liquid holdup was determined by a weighting method.

When gas and liquid were introduced into the column through flexible P.V.C. tubes, the excess weight over the dry column was weighted by a balance to within 2 g, and liquid holdup was determined after the weight of liquid contained in the entrance and exit tubes was subtracted.

Hydrocarbon liquid properties are presented in Table 2. In the presence of a gas flow rate, kerosene, desulfurized and nondesulfurized gas-oils have a tendency to foam which does not happen with cyclohexane, gasoline, and petroleum ether. However, it was not possible to characterize this by physicochemical parameters such as viscosity, density, and surface tension (see the comparable properties of cyclohexane and kerosene in Table 2). The gas were air, nitrogen, helium, and carbon dioxide ($0.15 < \rho_G < 2$ kg/m³). Superficial mass velocities of 0.5 to 15 kg/m² s and 0 to 1.5 kg/m² s for the liquid and the gas phases, respectively, were used to explore the whole field covered by the various hydrodynamic regimes.

FLOW PATTERNS

Several distinct flow patterns were observed when the liquid flow rate L was kept constant while the gas flow rate G was increased: trickling flow, pulsing flow, and sometimes spray flow for nonfoaming systems and trickling flow (when $G \simeq 0$); foaming flow, foaming pulsing flow, pulsing flow and spray flow for foaming systems. It is very im-

TABLE 2. COEFFICIENTS FOR NONCAPILLARY HOLDUP $\beta_{nc} = AL^a$

	Liquid	β_c	A	a	ρ_L, g/cm³	μ_L, cp	σ_L, dyn/cm
Glass spheres	Water	0.105	0.21	0.37	1	1.1	75
Spherical catalyst	Water	0.11	0.11	0.37	1	1.1	75
Spherical catalyst	Kerosene	0.077	0.26	0.53	0.79	0.99	25.3
Spherical catalyst	Cyclohexane	0.077	0.23	0.46	0.78	0.93	25
Cylindrical catalyst 1	Water	0.08	0.15	0.65	1	1.1	75
Cylindrical catalyst 2	Kerosene	0.077	0.40	0.35	0.79	0.99	25.3
Cylindrical catalyst 2	Cyclohexane	0.077	0.32	0.35	0.78	0.93	25
Cylindrical catalyst 2	Gasoline	0.077	0.31	0.36	0.84	0.57	25.2
Cylindrical catalyst 2	Desulfurized gas-oil	0.08	0.44	0.33	0.86	5	28.8
Cylindrical catalyst 2	Nondesulfurized gas oil	0.08	0.47	0.30	0.86	5	28.3
Cylindrical catalyst 2	Petroleum ether	0.06	0.40	0.40	0.65	0.31	19

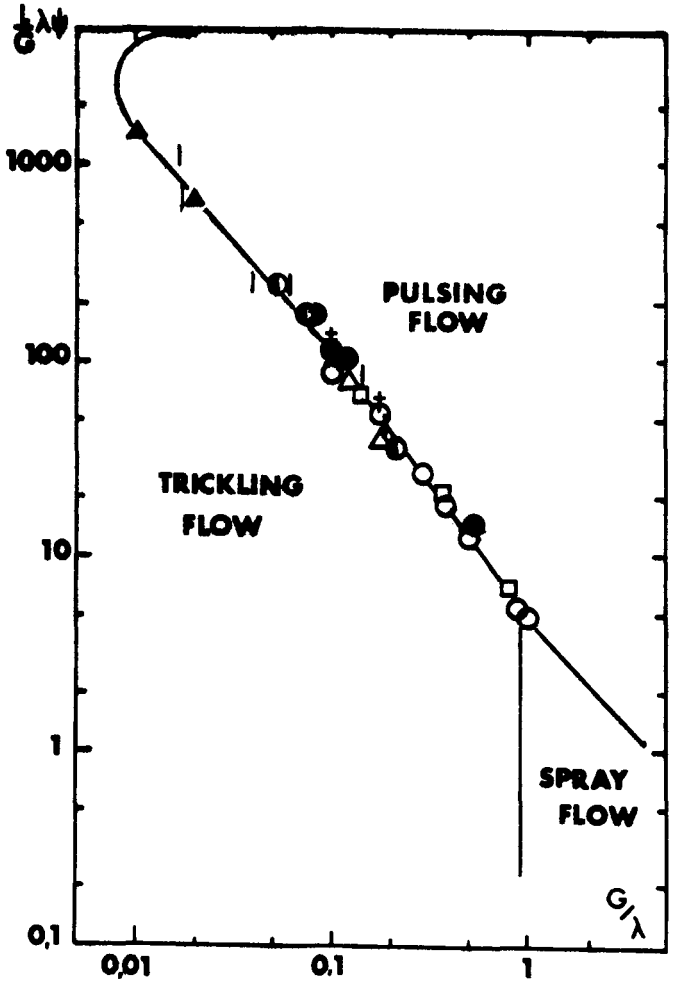

Fig. 1a. Flow Pattern Diagram for Nonfoaming Liquids.

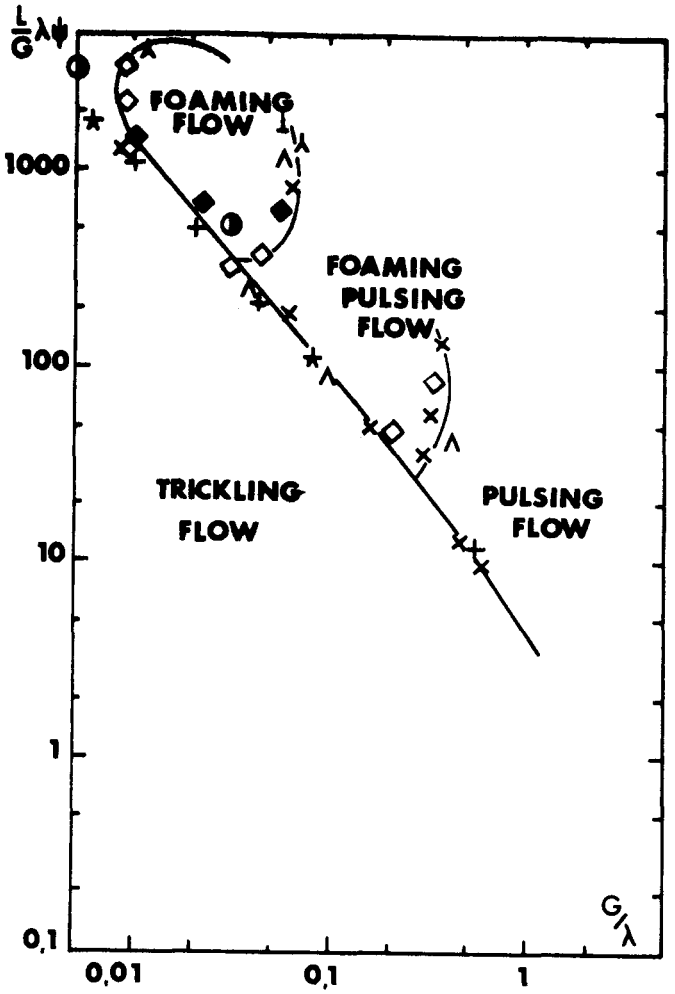

Fig. 1b. Flow Pattern Diagram for Foaming Liquids.

$$\lambda = \left[\frac{\rho G}{\rho_{wat}} \cdot \frac{\rho_L}{\rho_{air}}\right]^{0.5} \qquad \psi = \frac{\sigma_{wat}}{\sigma_L}\left[\frac{\mu_L}{\mu_{wat}}\left(\frac{\rho_{wat}}{\rho_L}\right)^2\right]^{0.33}$$

System	Packing	Key
Water-air	Spherical catalyst	○
Cyclohexane-air	Spherical catalyst	◐
Water-air	Cylindrical catalyst 1	□
Cyclohexane-nitrogen	Cylindrical catalyst 2	△
Gasoline-carbon dioxide	Cylindrical catalyst 2	●
Gasoline-nitrogen	Cylindrical catalyst 2	■
Gasoline-helium	Cylindrical catalyst 2	▲
Petroleum ether-nitrogen	Cylindrical catalyst 2	|
Petroleum ether carbon dioxide	Cylindrical catalyst 2	‡

System	Packing	Key
Kerosene-air	Spherical catalyst	◑
Desulfurized gas oil-carbon dioxide	Cylindrical catalyst 2	+
Desulfurized gas oil-air	Cylindrical catalyst 2	×
Desulfurized gas oil-helium	Cylindrical catalyst 2	⋏
Nondesulfurized gas oil-carbon dioxide	Cylindrical catalyst 2	⋆
Nondesulfurized gas oil-air	Cylindrical catalyst 2	⋀
Nondesulfurized gas oil-helium	Cylindrical catalyst 2	⊥
Kerosene-air	Cylindrical catalyst 2	◇
Kerosene-nitrogen	Cylindrical catalyst 2	◆

portant to note that before any data on hydrodynamic parameters such as liquid holdup or two-phase pressure drop are presented, it is absolutely necessary to characterize the flow patterns encountered.

Flow patterns and the transition from one configuration to another as a function of gas and liquid flow rates are described in Figures 1*a* and 1*b* for foaming and nonfoaming systems. The lines on these figures to separate the flow regimes are actually transition regimes rather than points of abrupt change from one flow type to another. It is worth noting that the line that separates trickling flow from the other flow regimes is the same in both diagrams. We generally consider it as the transition line between small gas-liquid interaction regime (trickling flow) and considerable gas-liquid interaction regime (foaming flow, foaming pulsing flow, pulsing flow, and spray flow) for reactors termed trickle-bed as defined by Satterfield (1975) and Charpentier et al. (1971). This transition line was previously obtained with air-water systems ($\lambda = \psi = 1$) for 3 mm packing in a 10 cm I.D. column by Charpentier et al. (1971).

LIQUID HOLDUP

The liquid holdup comprises the liquid held internally in the pores of the catalyst plus that outside the catalyst pellets. In this work, we are concerned with data of this external holdup β expressed as a fraction of the void volume between the catalyst particles. External holdup β is divided into free-draining or noncapillary holdup β_{nc} and residual or capillary holdup β_c. The capillary holdup varies typically from about 0.06 to about 0.11 for the liquids considered here. The experimental values of β_c for the hydrocarbons are well correlated by a relationship β_c vs. the Eotvos number Eo proposed by Charpentier et al. (1968). The noncapillary holdup is a function of the gas

and liquid flow rates, the catalyst characteristics, and the fluid properties.

For a zero gas flow rate, variations of β_{nc} with L are presented on Figure 2. As previously reported by different investigators, β_{nc} is correlated as proportional to L^a:

$$\beta_{nc} = AL^a \qquad (1)$$

with different values for coefficient a (Table 2). This result is not surprising because, for most of our experiments, the liquid is trickling over the packings in the shape of films, rivulets, and drops. Charpentier et al. (1968) have shown that a may vary between 0.33 to 0.66 for laminar to turbulent films, between 0.5 to 0.8 for laminar to turbulent rivulets, and $a = 1$ for drops. Therefore, for hydrocarbons systems, the exponents may be comprised between ideal values of 0.33 for laminar films over the packing and of 0.5 for laminar rivulets. Figure 2 shows also that data obtained with water are not representative of hydrocarbons data. Hydrocarbon noncapillary holdups are always much greater. Values of different coefficients to determine β_{nc} are presented in Table 2.

For the same hydrocarbon flow rate L, β_{nc} increases when surface tension decreases, when viscosity increases, and when the shape of the catalyst is cylindrical. In the viscosity range covered 0.31 to 5 cp, the exponent of 0.25 suggested by Satterfield and Way (1972) for the variations of β_{nc} with μ_L seems in reasonable agreement. Besides, it seems impossible to correlate with surface tension. Indeed, all other parameters being equal, it appears that for two hydrocarbons having the same surface tension, β_{nc} has quite different values following their tendency to foam or not.

In two-phase flow, for a given liquid flow rate, when we introduce and then increase a gas flow rate, the following trends are observed: for the nonfoaming liquids, β_{nc} keeps approximatively constant values for trickling flow, then decreases sharply with pulsing flow and slightly with spray flow when occurring (Charpentier et al., 1976); for the foaming liquids, β_{nc} keeps approximatively constant values for trickling flow, then decreases sharply with the foaming flow and pulsing foaming flow, then slightly increases or stays constant in the transition from pulsing foaming flow to pulsing flow, then decreases again with pulsing flow (Charpentier et al., 1976). The maximum in the holdup curves may be explained as the result of two opposite effects: an increasing pressure drop (and therefore a decreasing holdup) due to increasing gas flow rate and a decreasing pressure drop (and therefore an increasing holdup) due to increasing surface tension at the agitated liquid-gas interface where the dynamic surface tension is certainly higher than the static surface tension.

Indeed, the increasing gas rate increases the pressure drop and decreases the holdup as expected. However, an increasing gas flow rate also gives an increasing dynamic surface tension which decreases the stability of the foam bridging the packing channels, thus tending to increase the holdup. The net results of the opposite effects is to give a maximum as the gas flow rate is increased in the foaming pulsing region.

So, as a first approximation, Equation (1) is representative of the value of free-draining holdup for trickling flow (Figure 3). Gas phase and gas flow rate have a small influence on β_{nc}; that is, drag effects by the gas on the liquid are nonsignificant. Figure 3 is concerned with data representative of pilot plant reactors (Satterfield, 1975) for which it is quite sound to assume that the flow regime is a trickling flow of the liquid over the packing in the presence of a continuous gas phase. Actually this concerns a small range of gas flow rates G, this range becoming shorter as the liquid flow rate L increases.

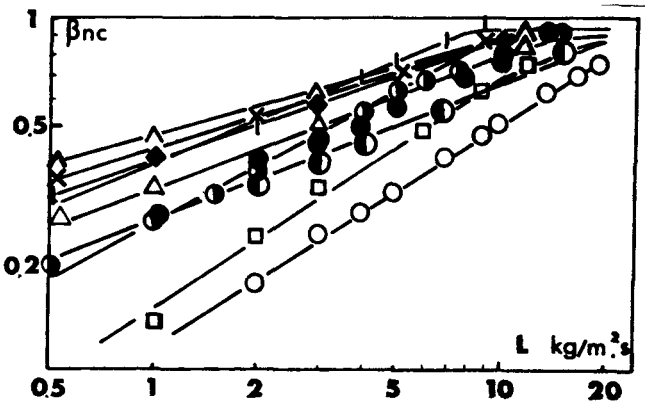

Fig. 2. Influence of Liquid Flow Rate on Noncapillary Liquid Holdup When $G = 0$.

System	Packing	Key
Water-air	Spherical catalyst	○
Cyclohexane-air	Spherical catalyst	◐
Kerosene-air	Spherical catalyst	◑
Water-air	Cylindrical catalyst 1	□
Cyclohexane-nitrogen	Cylindrical catalyst 2	△
Gasoline-air	Cylindrical catalyst 2	●
Desulfurized gas oil-air	Cylindrical catalyst 2	×
Nondesulfurized gas oil-air	Cylindrical catalyst 2	△
Kerosene-air	Cylindrical catalyst 2	◆
Petroleum ether-air	Cylindrical catalyst 2	|

For higher gas and liquid flow rates with other flow regimes as described on Figure 1, typical variations of β_{nc} with G are presented on Figure 4 for $L = 5$ kg/m² s. Curves going through a flat or having an S shape are representative of hydrocarbons already foaming for such a value of L. But generally foaming flow occurs for liquid flow rates higher than 5 kg/m² s, and holdup curves as well as pressure drop curves always go through a flat for the overall transition between foaming flow and pulsing flow, as explained above. Figure 4 is concerned with data representative of commercial reactors for which it does not seem quite sound to assume that the flow regime is a trickling flow but rather pulsing flow or foaming flow, and therefore the use of Equation (1) becomes irrelevant.

Larkins et al. (1961) reported holdup data including 3 mm glass spheres and 3 mm catalyst cylinders and correlated them in terms of a simple parameter χ as follows (with an average error of ± 20%):

$$\log \beta = -0.774 + 0.525 \log \chi - 0.109 (\log \chi)^2 \qquad (2)$$

$$\text{for} \quad 0.05 < \chi < 30$$

Here $\chi = (\Delta P_L / \Delta P_G)^{1/2}$, where ΔP_G is the single phase pressure loss for the gas flowing alone and ΔP_L for the liquid flowing alone with the same rate as those in two-phase flow. ΔP values are calculated by an Ergun's type of equation:

$$\frac{\Delta P}{Z} = h_k \frac{a_g^2 (1-\epsilon)^2}{\epsilon^3} \mu u + h_B \frac{a_g (1-\epsilon)}{\epsilon^3} \rho u^2 \qquad (3)$$

Values of h_k, h_B, and a_g for the packings of this study are presented in Table 1. Sato et al. (1973) reported data for 25.9 to 16.5 mm glass spheres and correlated them also in terms of the parameter χ and of a parameter a_s, taking into account a significant dependence of the specific surface area of beds:

$$\beta = 0.40\, a_s^{1/3}\, \chi^{0.22} \quad \text{for} \quad 0.1 < \chi < 20 \qquad (4)$$

with

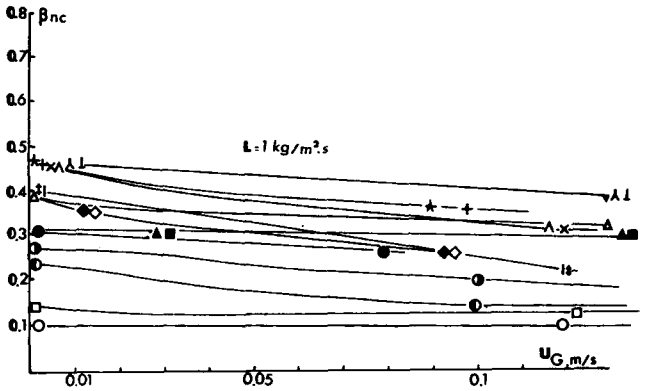

Fig. 3. Influence of Superficial Gas Velocity on Noncapillary Liquid Holdup When the Flow Pattern is Trickling Flow.

System	Packing	Key
Water-air	Spherical catalyst	○
Cyclohexane-air	Spherical catalyst	◐
Kerosene-air	Spherical catalyst	◑
Water-air	Cylindrical catalyst 1	□
Cyclohexane-nitrogen	Cylindrical catalyst 2	△
Gasoline-carbon dioxide	Cylindrical catalyst 2	●
Gasoline-nitrogen	Cylindrical catalyst 2	■
Gasoline-helium	Cylindrical catalyst 2	▲
Desulfurized gas oil-carbon dioxide	Cylindrical catalyst 2	+
Desulfurized gas oil-air	Cylindrical catalyst 2	×
Desulfurized gas oil-helium	Cylindrical catalyst 2	⅄
Nondesulfurized gas oil-carbon dioxide	Cylindrical catalyst 2	⅄
Nondesulfurized gas oil-air	Cylindrical catalyst 2	⋀
Nondesulfurized gas oil-helium	Cylindrical catalyst 2	⊥
Kerosene-air	Cylindrical catalyst 2	◇
Kerosene-nitrogen	Cylindrical catalyst 2	◆
Petroleum ether-nitrogen	Cylindrical catalyst 2	|
Petroleum ether-carbon dioxide	Cylindrical catalyst 2	‡

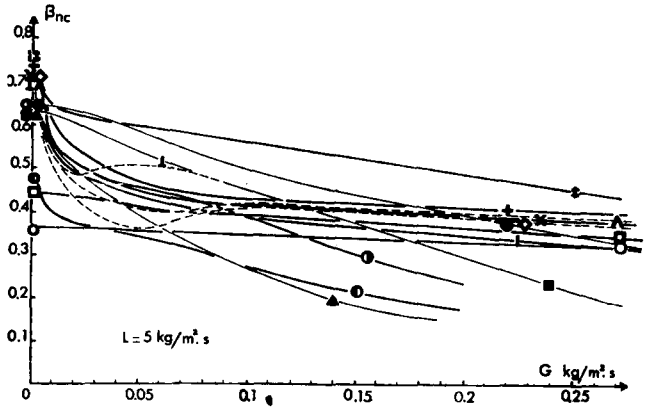

Fig. 4. Influence of the Gas Flow Rate on the Noncapillary Holdup.

System	Packing	Key
Water-air	Spherical catalyst	○
Cyclohexane-air	Spherical catalyst	◐
Kerosene-air	Spherical catalyst	◑
Water-air	Cylindrical catalyst 1	□
Gasoline-carbon dioxide	Cylindrical catalyst 2	●
Gasoline-nitrogen	Cylindrical catalyst 2	■
Gasoline-helium	Cylindrical catalyst 2	▲
Desulfurized gas oil-carbon dioxide	Cylindrical catalyst 2	+
Desulfurized gas oil-air	Cylindrical catalyst 2	×
Nondesulfurized gas oil-air	Cylindrical catalyst 2	⋀
Nondesulfurized gas oil-helium	Cylindrical catalyst 2	⊥
Kerosene-air	Cylindrical catalyst 2	◇
Petroleum ether-nitrogen	Cylindrical catalyst 2	|
Petroleum ether-carbon dioxide	Cylindrical catalyst 2	‡

$$a_s = \frac{6(1-\epsilon)}{d'} \quad \text{and} \quad d' = \frac{d}{1 + \dfrac{4d}{6D(1-\epsilon)}}$$

Bakos and Charpentier (1970) presented data for 3 mm glass spheres and catalyst spheres and underlined the fact that it is more relevant to use a parameter χ' relative to energy concept instead of momentum concept as it occurs with the parameter χ. They also claimed that one limiting case for such reactors is a trickling flow of liquid and not a single-phase flow of liquid, as it is assumed in the use of the parameter χ. Therefore, their equation was

$$\log \beta = P + Q \log \chi' + R(\log \chi')^2 \quad \text{for} \quad 0.05 < \chi' < 100 \tag{5}$$

with

$$\chi' = \left[\frac{\dfrac{L}{\epsilon \rho_m}}{\dfrac{G}{\epsilon \rho_m}\left[\dfrac{1}{\rho_G g_c} \cdot \dfrac{\Delta P_G}{Z} + 1\right]} \right]^{1/2}$$

$$\chi' = \left[\frac{\dfrac{L}{G}}{\dfrac{1}{\rho_G g_c} \cdot \dfrac{\Delta P_G}{Z} + 1} \right]^{1/2}$$

χ' being the square root of the ratio of the specific flux of frictional energy dissipated when liquid is trickling on the packing to that when the gas is flowing through the packing (Charpentier et al., 1971). For example, values of $P = -0.280$, $Q = 0.175$, and $R = -0.047$ were given for spherical packing.

It is important to note that Equations (2), (4), and (5) are relative to data reported from measurements of air-water systems.

On Figures 5 and 6 present data are compared with these three types of correlations for $L = 1$ and 5 kg/m² s and for twenty gas-liquid systems studied. Larkin's correlation does not fit the data, which is not surprising because it does not concern results reported from experimental measurements with hydrocarbons. The fit is better with Sato's correlation, though it is substantially higher. The best line representing our results with the majority of data for cylindrical catalyst is (with an average of ± 20%)

$$\log \beta = -0.363 + 0.168 \log \chi' - 0.043 (\log \chi')^2 \quad \text{for} \quad 0.05 < \chi' < 100 \tag{6}$$

Data for spherical catalyst are best correlated by Equation (5), with coefficients P, Q, and R relative to spherical packings.

Over 1 500 data points are presented on Figures 5 and 6, though many have been omitted for clarity. As previously said, the data concerning water as liquid phase are not correlated, especially for trickling flow regime (Figure 5). It is important to note that Equation (6) fits experimental results relative to a large range of hydrocarbon liquids.

In conclusion, for design purpose, Sato's relationship or Equations (5) or (6) may be used to determine holdup data for foaming and nonfoaming hydrocarbons and for any flow regime with catalyst packings. The only empiricism involved is that required in correlating pressure drop when one or both phases are flowing alone. Our own experience led us to insist on the fact that this should be quickly determined experimentally in a small column packed with the catalyst to be used (for example, see in

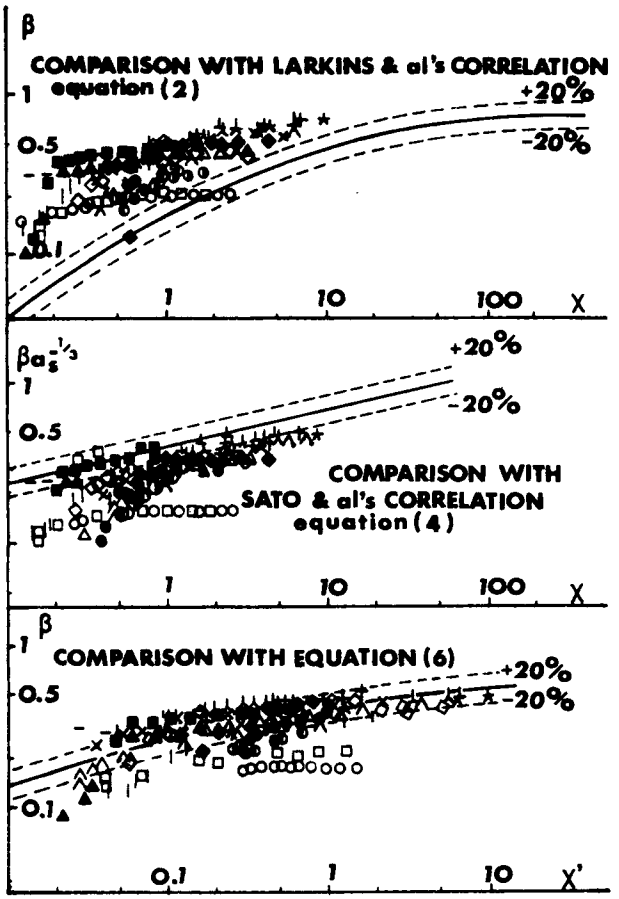

Fig. 5. Comparison of Total Liquid Holdup with Predictive Correlations for $L = 1$ kg/m^2 s.

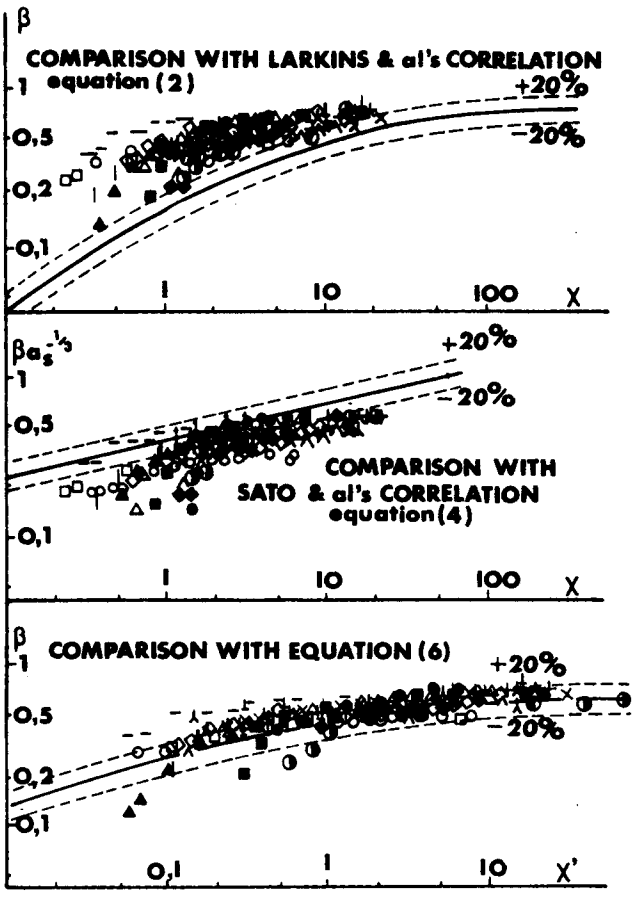

Fig. 6. Comparison of Total Liquid Holdup with Predictive Correlations for $L = 5$ kg/m^2 s.

System	Packing	Key
Water-air	Spherical catalyst and glass spheres in a 10cm J.D. column	—
Water-air	Spherical catalyst	○
Cyclohexane-air	Spherical catalyst	◐
Kerosene-air	Spherical catalyst	◑
Water-air	Cylindrical catalyst 1	□
Cyclohexane-nitrogen	Cylindrical catalyst 2	△
Gasoline-carbon dioxide	Cylindrical catalyst 2	●
Gasoline-nitrogen	Cylindrical catalyst 2	■
Gasoline-helium	Cylindrical catalyst 2	▲
Desulfurized gas oil-carbon dioxide	Cylindrical catalyst 2	+
Desulfurized gas oil-air	Cylindrical catalyst 2	×
Desulfurized gas oil-helium	Cylindrical catalyst 2	⅄
Nondesulfurized gas oil-carbon dioxide	Cylindrical catalyst 2	⅄
Nondesulfurized gas oil-air	Cylindrical catalyst 2	⋀
Nondesulfurized gas oil-helium	Cylindrical catalyst 2	⊥
Kerosene-air	Cylindrical catalyst 2	◇
Kerosene-nitrogen	Cylindrical catalyst 2	◆
Petroleum ether-nitrogen	Cylindrical catalyst 2	|
Petroleum ether-carbon dioxide	Cylindrical catalyst 2	‡

Table 1 the different values of h_k and h_B for the different packings).

Equation (1) is an alternative relationship for very small gas flow rates in the range of those used in the laboratory scale petroleum refining studies. However, it must be known that this equation fails completely for the prediction of commercial operations holdup because the gas flow rates are often much higher and therefore the holdup is much smaller.

ACKNOWLEDGMENT

The authors wish to acknowledge Miss E. Hanel and M. J. Gyenis for their excellent experimental work during this study and the Institut Français du Petrole for the financial support and the permission to publish this note.

NOTATIONS

A = coefficient in Equation (1)
a = exponent in Equation (1)
a_g = specific surface area of the packing
D = column diameter
d = particle diameter
Eo = Eotvos number, $(\rho_L g_c d^2)/(\sigma_L)$
G = superficial gas flow rate
g_c = conversion constant
h_k, h_B = constants in Equation (5)
L = superficial liquid flow rate
P, Q, R = coefficients in Equation (5)
u_G = gas superficial velocity
Z = height of packed bed

Greek Letters

β, β_{nc}, β_c = total, noncapillary and capillary holdup expressed in percentage of interparticle void $\beta = \beta_{nc} + \beta_c$
ΔP = pressure loss; ΔP_L for single phase liquid, ΔP_G for single phase flow
ϵ = porosity (interparticle)
λ = flow parameter, $\lambda = \left[\frac{\rho_G}{\rho_{air}} \cdot \frac{\rho_L}{\rho_{wat}}\right]^{0.5}$
μ_G, μ_L, μ_{wat} = gas, liquid viscosity, and water viscosity
ρ_G, ρ_L, ρ_{wat}, ρ_m = gas, liquid, water, manometric fluid density
σ_L, σ_{wat} = liquid, water surface tension
ψ = flow parameter,

$$\psi = \frac{\sigma_{wat}}{\sigma_L}\left[\frac{\mu_L}{\mu_{wat}}\left[\frac{\rho_{wat}}{\rho_L}\right]^2\right]^{0.33}$$

LITERATURE CITED

Bakos, M., and J. C. Charpentier, "Taux de Rétention pour des écoulements gaz-liquide à Cocourant vers le Bas dans les colonnes à Garnissage Arrosé et Noyé," *Chem. Eng. Sci.*, **25**, 1822 (1970).

Charpentier, J. C., C. Prost, W. P. M. Van Swaaij, and P. Le Goff, "Etude de la Rétention de liquide dans une colonne à garnissage arrosé à contre-courant et à co-courant de gaz-liquide," *Chim. Ind. Génie Chim.*, 99, 803 (1968).

Charpentier, J. C., C. Prost and P. Le Goff, "Ecoulement Ruisselant de Liquide dans une colonne à garnissage. Détermination des Vitesses et des Débits Relatifs des Films, des Filets et des Gouttes," *ibid.*, **100**, 653 (1968).

Charpentier, J. C., M. Bakos, and P. Le Goff, "Hydrodynamics of Two-Phase Concurrent Downflow in Packed Bed Reactors," paper presented at the 2nd Congr. on "Quelques applications de la Chimie Physique," Veszprem, Hungary (1971).

Charpentier, J. C., N. Midoux, and M. Favier, "Hydrodynamics of Concurrent Two Phase Downflow in Packed Bed Reactors," *Chem. Eng. Sci.*, to be published.

Henry, H. C., and J. B. Gilbert, "Scale Up of Pilot Plant Data for Catalytic Hydroprocessing," *Ind. Eng. Chem. Process Design Develop.*, **12**, 328 (1973).

Larkins, R. P., R. R. White, and D. W. Jeffrey, "Two-Phase Concurrent Flow in Packed Beds," *AIChE J.*, **7**, 231 (1961).

Mears, D. E., "The Role of Liquid Holdup and Effective Wetting in the Performance of Trickle Bed Reactors," *Chem. Reaction Eng.*, **2**, Adv. in Chem. Ser. No. 133, p. 218 (1974).

Sato, Y., T. Hirose, F. Takahashi, and M. Toda, "Pressure Loss and Liquid Hold Up in Packed Bed Reactor with Co-current Gas-Liquid Down Flow," *J. Chem. Eng. Japan*, **6**, 315 (1973).

Satterfield, C. N., and P. F. Way, "The Role of the Liquid Phase in the Performance of a Tricke-Bed Reactor," *AIChE J.*, **18**, 305 (1972).

Satterfield, C. N., and F. Ozel, "Direct Solid Catalyzed Reaction of a Vapor in an Apparently Completely Wetted Trickle-Bed Reactor," *ibid.*, **19**, 1259 (1973).

Satterfield, C. N., "Tricke-Bed Reactors," *ibid.*, **21**, 209 (1975).

Wijffels, J. B., J. Verloop, and J. F. Zuiderweg, "On the Wetting of Catalyst Particles under Trickle Flow Conditions," *Chem. Reaction. Eng.*, **2**, Adv. Ser. No. 133, p. 151 (1974).

Manuscript received July 7, 1975; revision received September 5 and accepted September 9, 1975.

Prediction of the Pressure Drop Across Sieve Trays

CHRIS A. E. DAVY and GEOFFREY G. HASELDEN

Department of Chemical Engineering
University of Leeds, Leeds, England

Generally, the total pressure drop across a sieve tray operating in the froth regime is calculated as the sum of a number of terms representing additive resistances to vapor flow:

$$P = h_{DT} + h_v$$

Although it is generally recognized that the pressure drop across the tray itself is not the same with and without liquid, in nearly all cases this assumption is made, and any variations due to the presence of liquid on the tray are incorporated in an additional term such that $h_v = h_L + h_R$.

Many suggestions have been made regarding the value of h_R (Hunt et al., 1955; Mayfield et al., 1952; and Brambilla et al., 1969). However, it will be contended that this approach is unsound, since vapor flow through the holes on the tray is fundamentally modified owing to the presence of liquid for the following reasons:

1. Not all the holes have an equal, instantaneous vapor flow rate. Owing to the irregular movement of liquid across the floor of the tray, some holes, or groups of holes, may be discharging rapidly at a given instant, while others may be temporarily inactive.

2. The rate of flow through an individual hole is oscillatory as bubbles grow and then detach.

3. Liquid may penetrate into the holes, effectively reducing the area available for vapor flow. At high vapor velocities, this penetration may depend on surface tension forces, but as the vapor velocity through the holes decreases, the liquid penetration can rapidly increase owing to gravity. This is the situation when the tray is weeping.

4. There is a venturi effect produced by the cone of liquid around the gas stream at the outlet of each hole which will tend to decrease the pressure drop and could give rise to pressure recovery. This is likely to be most noticeable at high hole velocities when the gas emerges from the holes nearly continuously rather than as distinct bubbles.

Steiner and Kolar (1969) have recognized that any equation for dry tray pressure drop must be modified for